Proceedings of the 17th World Congress
The International Federation of Automatic Control
Seoul, Korea, July 6-11, 2008

Vss Speed Sensorless Control of PMSM

Karel Jezernik

University of Maribor, Faculty of Electrical Engineering and Computer Science,
Smetanova ul. 17, 2000 Maribor, Slovenia
(Tel.: +386-2-220 73 00, e-mail: karel.jezernik@uni-mb.si)

Abstract: The speed sensorless control of nonsalient PMSM that uses estimated rotor flux instead of the transformation angle is designed. This paper introduces a new sequential switching control strategy for a current control of a three phase inverter. The key idea is to integrate the benefits of the variable structure system control design and the event-driven sequential control structures to raise the system performance and control efficiency. The design is applied to the control of three phase permanent magnet synchronous machine. The operation at low speed is improved by reducing the disturbance impact. The estimation angle error at zero speed is limited by injecting the DC current that compensates the unknown load torque and enables operation at zero speed. The VSS speed sensorless control of PMSM is implemented on a DSP/FPGA system, and verified experimentally.

1. INTRODUCTION

Modern Synchronous Motors with Permanent Magnets (PMSM), combined with the advanced control techniques are used as high performance drives, capable of four quadrant operation. The motor properties, such as smooth output torque, low harmonics, torque/volume ratio, high output power and efficiency, can be improved by using high quality magnets along with the construction solutions, in many cases resulting to almost ideal nonsalient drives (Leonhard).

The vector control of synchronous motor requires information of rotor flux, since it is strongly connected to the produced torque. Rotor flux angle is normally obtained by using mechanical rotor position sensor still indispensable in robust, high performance drives. Sensorless techniques usually extract rotor flux information from measured electrical quantities, especially from stator voltage and stator current in order to improve reliability and reduce manufacturing costs (Holtz). Many approaches are reported in the literature, using one or the combination of the following principles (Bolognani *et al.*):

- Extracting motional EMF,
- Using third harmonic of motional EMF,
- Inductance variation techniques by injection high frequency signal,
- Integration the flux linkage variation.

Recent theoretical advances in the field of hybrid and discrete event-systems, and significant increase of the computational power available for the control of the power electronic systems are inviting both the control and the power electronics communities to adopt traditional control schemes associated with power electronics applications. In order to raise the performance and efficiency of the drive applications, faster and more sophisticated current control schemes are required.

In this paper, the conventional current control scheme consisting of discrete-time current controller and pulse-width modulator is replaced with the new sequential switching current control strategy. Inherent switching operation of the three phase bridge requires adopted control principles. Hysteresis controllers can be a good alternative for such applications. They are robust to system parameter variations, exhibit very good dynamics, require simple implementation and enable direct control of the bridge transistors without special modulators. Their main drawback is a limited control of transistor switching frequency. Usually, three independent hysteresis controllers for a three phase bridge are used. On the other hand, multivariable hysteresis current control structures are complex and therefore less used in current control structures. Introduction of switching pattern sequence can be a good alternative for the switching frequency reduction. However, the lack of systematic methodologies brings the problems to the sequential hysteresis current controller design, analysis and implementation level (Rossi *et al.*), (Tilli *et al.*).

In order to preserve the benefits of the hysteresis current control approach on one hand and to limit the switching frequency on the other hand, a twofold design approach is proposed in this paper. The Lyapunov stability condition determination from the variable structure system control theory is introduced first and recursive description of event driven systems for determination of switching sequence is applied next. The Lyapunov stability condition determination yields the switching conditions for the transfer among the discrete states of the switching sequence.

2. MACHINE DYNAMICS AND PROBLEM STATEMENT

2.1 PMSM Model

The model of the control object, the nonsalient PMSM in the stationary stator frame, is expressed by complex notation as:

$$\boldsymbol{u}_s = R_s \boldsymbol{i}_s + d\boldsymbol{\Psi}_s / dt , \quad (1)$$

$$\boldsymbol{\Psi}_s = \boldsymbol{\Psi}_r + L_s \boldsymbol{i}_s , \quad (2)$$

$$\boldsymbol{\Psi}_r = \Psi_{PM} e^{j\Theta} , \quad (3)$$

$$J\, d\omega / dt = T_e - T_l , \quad (4)$$

$$d\Theta / dt = p\omega , \quad (5)$$

$$T_e = (3p/2)(\boldsymbol{\Psi}_r \otimes \boldsymbol{i}_s) = 1.5p(\Psi_{ra} i_{sb} - \Psi_{rb} i_{sa}) , \quad (6)$$

where ω is the mechanical rotor angle speed, complex variables $\boldsymbol{u}_s = u_{sa} + ju_{sb}$, $\boldsymbol{i}_s = i_{sa} + ji_{sb}$, $\boldsymbol{\Psi}_r = \Psi_{ra} + j\Psi_{rb}$ are stator voltage, stator current and rotor flux, respectively. T_e is motor torque, T_l is load torque, *J* is inertia of the rotor with load and p is the number of pole pairs. Motor torque T_e is expressed as vector product $\otimes$ between rotor flux and stator current

2.2. Proposed Control Scheme

The design of sliding mode system consists generally of two-step procedure: design of the switching manifold and design of the sliding mode control algorithm. The switching manifold shall be selected in such a way to guaranty desired system performance while the control shall be selected to ensure that system's motion is forced to stay in sliding mode manifold. Mathematically above procedure may be presented as follows (Utkin):

1) From the system specification select the vector valued function $\boldsymbol{\sigma} = \boldsymbol{\sigma}(\boldsymbol{x}^r, \boldsymbol{x})$ where $\boldsymbol{x}^r$ represent desired changes of the controlled vector variable $\boldsymbol{x}$ so that the design specifications are met if the closed loop system is constrained to belong to the manifold (7)

$$\boldsymbol{S} = \left\{ \boldsymbol{x} : \boldsymbol{\sigma} = \boldsymbol{\sigma}(\boldsymbol{x}^r, \boldsymbol{x}) = \boldsymbol{0} \right\} . \quad (7)$$

This way the fulfillment of the control system design specifications is reduced selection of control that will guaranty the stability of the system.

2) The control input shall be selected so that the stability of the solution $\boldsymbol{\sigma} = \boldsymbol{\sigma}(\boldsymbol{x}^r, \boldsymbol{x})$ is guarantied. The simplest approach is to use Lyapunov based design in such a way that the control is determined from the Lyapunov stability conditions. Since fulfillment of the design requirements is reduced to the stability of (7) natural selection of the Lyapunov function candidate is in the following form

$$V = -\boldsymbol{\sigma}^T \boldsymbol{\sigma} / 2 \quad \text{and} \quad \dot{V} = \boldsymbol{\sigma}^T \dot{\boldsymbol{\sigma}} . \quad (8)$$

The Lyapunov stability requirement will be fulfilled if control can be selected such that $\dot{V}\big|_{\forall\sigma\neq 0} < 0$ and $\dot{V}\big|_{\sigma=0} = 0$. This can be achieved if the following is satisfied (a) the derivative $\dot{V}$ of the Lyapunov function is function of control and (b) there is such a function $\boldsymbol{\Phi}(\boldsymbol{\sigma})$ so that $\boldsymbol{\sigma}^T \boldsymbol{\Phi}(\boldsymbol{\sigma})\big|_{\forall\sigma\neq 0} < 0$ and (c) if there is unique solution for control for the following equality

$$\dot{V} = \boldsymbol{\sigma}^T \dot{\boldsymbol{\sigma}}(\boldsymbol{u}) = \boldsymbol{\sigma}^T \Phi(\boldsymbol{\sigma}) < 0 . \quad (9)$$

There can be many different ways of selecting function $\boldsymbol{\Phi}(\boldsymbol{\sigma})$. For the application in electrical drive control two particular forms as given in (10) may be of interest:

$$\dot{V} = \boldsymbol{\sigma}^T \boldsymbol{\Phi}(\boldsymbol{\sigma}) < 0 \Rightarrow \begin{cases} \boldsymbol{\Phi}(\boldsymbol{\sigma}) = -\boldsymbol{\Gamma} sign(\boldsymbol{\sigma}) & ...a) \\ \boldsymbol{\Phi}(\boldsymbol{\sigma}) = -\boldsymbol{D}\boldsymbol{\sigma}; \boldsymbol{D} > \boldsymbol{0} & ...b) \end{cases} \quad (10)$$

where $\boldsymbol{\Gamma}$ is diagonal or matrix with predominant diagonal, $sign(\boldsymbol{\sigma}) = \left[sign(\sigma)_1, \cdots, sign(\sigma_m) \right]^T$ and $\mathbf{D}$ is positive definite matrix.

If vector function $\boldsymbol{\Phi}(\boldsymbol{\sigma})$ is selected to be $\boldsymbol{\Phi}(\boldsymbol{\sigma}) = -\boldsymbol{\Gamma} sign(\boldsymbol{\sigma})$ then resulting control will be discontinuous and manifold will be reached in finite time. If $\boldsymbol{\Phi}(\boldsymbol{\sigma})$ is selected as $\boldsymbol{\Phi}(\boldsymbol{\sigma}) = -\boldsymbol{D}\boldsymbol{\sigma}; \boldsymbol{D} > \boldsymbol{0}$ then resulting control is expected to be continuous and sliding mode manifold will be reached in infinite time. The asymptotic stability of the solution $\boldsymbol{\sigma} = \boldsymbol{\sigma}(\boldsymbol{x}^r, \boldsymbol{x}) = \boldsymbol{0}$ will be guarantied in this case. Both solutions may be applied to the electrical motor control.

The so called discontinuous control (10a) will be applied in stator current switching control (Section 3). The continuous control (10b) will be implemented for rotor flux observer (Section 4). Switching control is natural principle in inverter, but observer structure requested continuous output function, i.e. estimated rotor flux.

3. SEQUENTIAL SWITCHING CURRENT CONTROL DESIGN

Fig. 1 shows the torque and speed sensorless control of PMSM. The considered control problem is tracking of a three-phase current reference signal. Controller input and output signals are logical variables indicating the driving status of inverter switches, as a consequence, the dynamic controller can be designed as a finite-state automation or Petri net state model, suitable for very fast and low cost FPGA implementation. The FPGA based solution allows simultaneous execution of all control procedures, like start up, steering and protection which can be added with an additional resources and almost no drawback in performance.

To control the drive current, the sector of drive voltage $\boldsymbol{u}_s$ is recognized first, and based on the known sector, the output voltage vector (the transistor switching pattern) for the drive current control is selected respecting the current control error related with Lyapunov stability condition. Considering space vector representation of the drive stator voltage $\boldsymbol{u}_s$, the voltage is represented as vector rotating around the origin. Six active switching vectors of the three phase transistor bridge result six output voltage vectors denoted $\boldsymbol{v}_1 ... \boldsymbol{v}_6$. According to the signs of the phase voltages u_{s1}, u_{s2} and u_{s3}, the phase plane is divided into six sectors denoted Sect 1 … Sect 6 (Polic *at al.*).

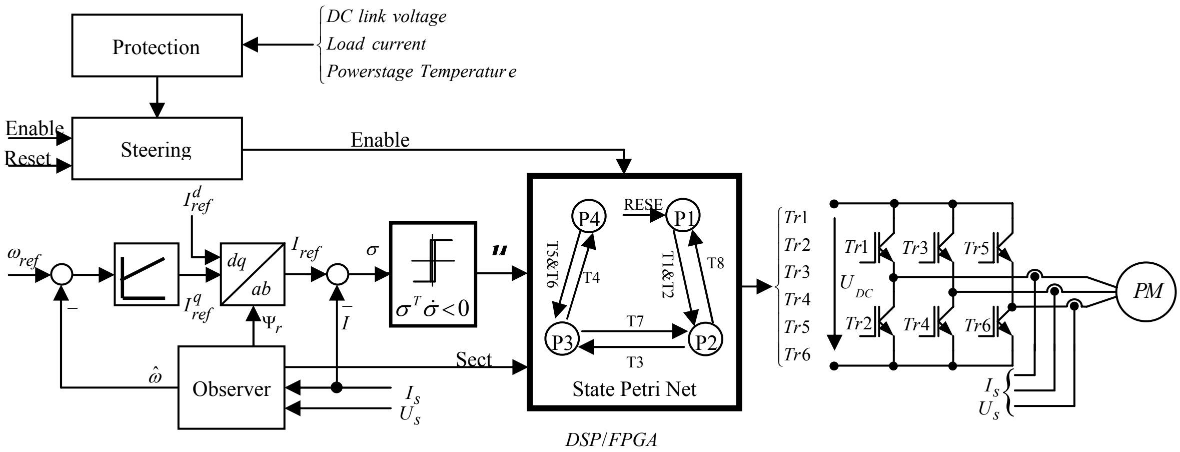

Fig. 1: Block diagram of event-driven sliding mode control of PM.

Switching among the available output voltage vectors in each sector are determined by the conditions originate from the derivative of the Lyapunov function. For the Lyapunov function candidate

$$V = (1/2)\boldsymbol{\sigma}^T\boldsymbol{\sigma} = (1/2)\left(\boldsymbol{i}_s^d - \boldsymbol{i}_s\right)^T\left(\boldsymbol{i}_s^d - \boldsymbol{i}_s\right), \quad (11)$$

the stability requirement will be fulfilled if control can be selected such, that the derivative of the Layapunov function candidate is negative $\dot{V} = \boldsymbol{\sigma}^T\dot{\boldsymbol{\sigma}} \le 0$. Derivatives of current control error (11) may be expressed with voltage equation $(d/dt)\left(\boldsymbol{i}_s^d - \boldsymbol{i}_s\right) = (d/dt)\boldsymbol{i}_s^d - (1/L_s)\left(\boldsymbol{u}_s - R_s\boldsymbol{i}_s - \boldsymbol{e}_r\right)$, where $\boldsymbol{i}_s^d$, $\boldsymbol{i}_s$ are desired and actual stator current of motor, $\boldsymbol{u}_s$ is voltage control input, $R_s\boldsymbol{i}_s$ is resistive voltage drop and $\boldsymbol{e}_r$ is EMF of the motor. The conditions for the sequential switching of the power inverter are selected as:

$$S_R = (1/2)(1-\operatorname{sign}(A)),\ S_S = (1/2)(1-\operatorname{sign}(B)),$$
$$S_T = (1/2)(1-\operatorname{sign}(C)) \quad (12)$$

where

$$A = \left(i_{sa}^d - i_{sa}\right)$$
$$B = -(1/2)\left(i_{sa}^d - i_{sa}\right) - (\sqrt{3}/2)\left(i_{sb}^d - i_{sb}\right), \quad (13)$$
$$C = -(1/2)\left(i_{sa}^d - i_{sa}\right) + (\sqrt{3}/2)\left(i_{sb}^d - i_{sb}\right)$$

which is evolved from the Lyapunov function derivative. When U_{DC} has enough magnitude that $\dot{V} \le 0$, than $V \to 0$ and $\boldsymbol{i}_s \to \boldsymbol{i}_s^d$. Notice that if S_R, S_S, S_T equal to zero simultaneously, no current is delivered to the motor.

The PN-graph can be described in the matrix based recursive form. The proposed design has inputs $\boldsymbol{u}$, events $\boldsymbol{x}$, discrete states $\boldsymbol{m}$ and outputs $\boldsymbol{y}$ denoted by logical vectors. $\boldsymbol{m}_0$ denotes initial discrete state (Fig. 2).

Inputs $\boldsymbol{u}$ denotes switching conditions S_R, S_S, S_T of the Laypunov stability criteria and signs of the drive stator phase voltages u_{s1} , u_{s2} and u_{s3}, where $sign(x)$ = 1 denotes positive and sign(x) = 0 negative values. Events $\boldsymbol{x}$ denote conditions for occurrence of transitions among discrete states. Discrete states $\boldsymbol{m}$ correspond to the appropriate output voltage vectors and outputs $\boldsymbol{y}$ denote the transistor gate signals for the generation of corresponding output voltage vectors.

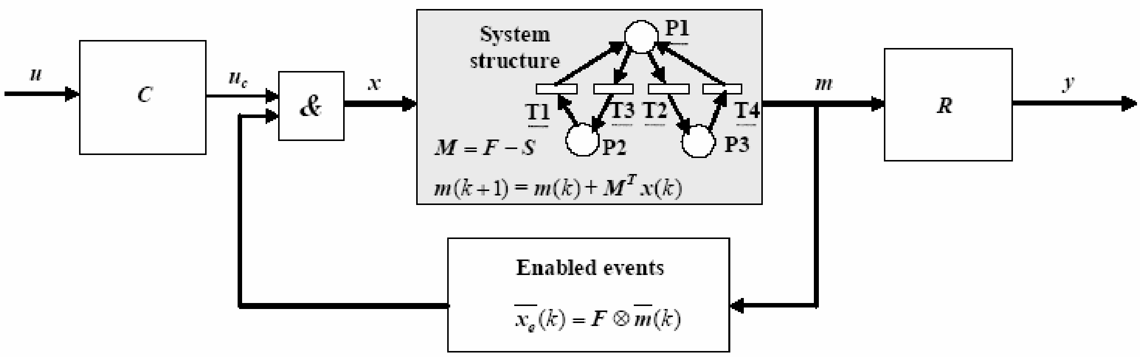

Fig. 2: Recursive description of event driven systems.

$$\boldsymbol{u}=\begin{bmatrix} S_R \\ S_S \\ S_T \\ \mathrm{sign}(u_{s1}) \\ \mathrm{sign}(u_{s2}) \\ \mathrm{sign}(u_{s3}) \end{bmatrix}, \boldsymbol{x}=\begin{bmatrix} T_1 \\ T_2 \\ T_3 \\ T_4 \\ T_5 \\ T_6 \\ T_7 \\ T_8 \end{bmatrix}, \begin{matrix} \boldsymbol{m}=\begin{bmatrix} P_1 \\ P_2 \\ P_3 \\ P_4 \end{bmatrix} \\ \boldsymbol{m}_0=\begin{bmatrix} 1 \\ 0 \\ 0 \\ 0 \end{bmatrix} \end{matrix}, \boldsymbol{y}=\begin{bmatrix} Tr_1 \\ Tr_2 \\ Tr_3 \\ Tr_4 \\ Tr_5 \\ Tr_6 \end{bmatrix}. \quad (14)$$

The reference current can now be calculated simply as:

$$\boldsymbol{i}_s^d=\left(1/\left|\hat{\boldsymbol{\Psi}}_r\right|\right)\left(\hat{\boldsymbol{\Psi}}_r\odot\boldsymbol{i}_s\right)+j2/\left(3p\left|\hat{\boldsymbol{\Psi}}_r\right|\right)\left(T_e^d/\Psi_{PM}\right). \quad (15)$$

A common used dq-ab transformation in conventional current control, the components of the rotor flux are directly employed as:

$$e^{j\Theta}=\cos\Theta+j\sin\Theta=\hat{\Psi}_{ra}/\left|\hat{\boldsymbol{\Psi}}_r\right|+j\hat{\Psi}_{rb}/\left|\hat{\boldsymbol{\Psi}}_r\right|=\hat{\boldsymbol{\Psi}}_r/\left|\hat{\boldsymbol{\Psi}}_r\right|. \quad (16)$$

The advantage of proposed transformation is that the sin and cos function are replacement with multiplication in algoritm. Further algorithm simplification can be made with replacement $\left|\hat{\boldsymbol{\Psi}}_r\right|\approx\Psi_{PM}$ due permanent magnet $\Psi_{PM}=\mathrm{const}$.

4. ROTOR FLUX OBSERVER

4.1 Design Procedure

This rotor flux observer, is based on the stator equation (1), where the derivative of the estimated stator flux is calculated from measured stator voltage and current. The observer equation (17) represents the first order vectorial differential equation. The stator voltage $\boldsymbol{u}_s$ and current $\boldsymbol{i}_s$ serve as control input to the estimated stator flux $\hat{\boldsymbol{\Psi}}_s$. The measured value of the stator voltage is used instead of the commonly used reference voltage, in order to avoid voltage error influence due to power-stage non-linear behavior:

$$(d/dt)\hat{\boldsymbol{\Psi}}_s=\hat{\boldsymbol{u}}_s-\hat{R}_s\boldsymbol{i}_s+\hat{\boldsymbol{u}}_k, \quad (17)$$

$$\hat{\boldsymbol{u}}_k=\hat{\boldsymbol{\Psi}}_r\left(u_m+ju_p\right). \quad (18)$$

Non-modeled dynamic is set as a remaining signal $\hat{\boldsymbol{u}}_k$, calculated from the magnitude error of the rotor flux $\left|\Delta\boldsymbol{\Psi}_r\right|$. The stator parameters of the PMSM appear in the rotor flux observer; i.e. stator resistance $\hat{R}_s$ and stator inductance $\hat{L}_s$. The influence of the stator inductance variation is small, but stator resistance changes significantly during the operation. The variation of the stator resistance $\Delta\hat{R}_s$ impacts on the estimated rotor flux and, due to this, on the variation of the PMSM's torque.

The influence of the rotor flux variation's magnitude is compensated by introducing a non-linear magnitude and orientation feedback compensator in the observer. The switching function of the VSC flux magnitude controller C_m is set to the error between the reference and estimated rotor flux magnitude:

$$\left(d\sigma_m/dt\right)=D_m\sigma_m=0,\quad \sigma_m=\Psi_{PM}-\left|\hat{\boldsymbol{\Psi}}_r\right|. \quad (19)$$

The discrete part of the resulting unknown offset voltage u_m is:

$$C_m: u_m(k)=\left(K_m/T_s\right)\left(\left(1+T_sD_m\right)\sigma_m(k)-\sigma_m(k-1)\right). \quad (20)$$

Furthermore, the variation of the stator resistance $\Delta\hat{R}_s$ impacts to the torque variation of the PMSM, expressed by the variation of the rotor flux $u_m(k)$, desired torque T_e^d and flux Ψ_{PM}:

$$\Delta T_e=u_m(k)\,T_e^d/\Psi_{PM}. \quad (21)$$

Torque variation will induce variation of speed $\Delta\omega$ of PMSM with taking into account mechanical model of machine (4):

$$u_p=\frac{1}{J}\int_0^t\Delta T_e\,d\tau \quad (22)$$

The source of the connection between the torque error and the rotor flux error is the influence of the stator resistance error, when the torque is applied.

Correction input signals u_m and u_p, influence the magnitude and orientation of the magnetic flux error, make the proposed observer robust to the parameter uncertainties variations. The resulting diagram of both, an amplitude and phase-controlled, variable frequency two phase oscillator is shown in Fig. 3, which is suitable for providing the estimated stator and rotor fluxes of the PMSM.

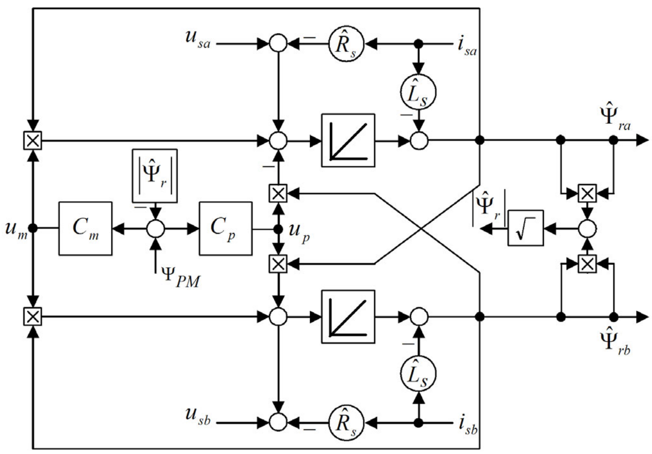

Fig. 3: Block diagram of the rotor flux observer represented as two phase oscillator.

The estimate of the EMC, used in the current controller, can be expressed by using estimated speed and estimated rotor flux:

$$\hat{e}_r = p\hat{\omega}\left(-\hat{\Psi}_{rb} + j\hat{\Psi}_{ra}\right). \quad (23)$$

The estimated speed is computed entirely from the estimated rotor flux and it's time derivative:

$$\hat{\omega} = p^{-1}\left(\hat{\boldsymbol{\Psi}}_r \otimes (d/dt)\hat{\boldsymbol{\Psi}}_r\right)/\left|\hat{\boldsymbol{\Psi}}_r\right|^2. \quad (24)$$

The resulting estimated speed is subjected to high noise levels due to the derivative term that can be reduced by employing low pass filters.

4.2 Stability of Rotor Flux Observer

The stability is computed only for magnitude rotor flux error, which is common input for both, the magnitude and orientation errors of rotor flux observer. A Lyapunov stability criteria is used, to verify the stability of the observer. The squared magnitude of the rotor flux error is set as a Lyapunov candidate function. In the selected case, a Lyapunov candidate function is, as required, always positive. The notation is adopted for complex numbers.

$$V = (1/2)\,\mathrm{Re}\left\{\left(\hat{\boldsymbol{\Psi}}_r - \boldsymbol{\Psi}_r\right)\left(\hat{\boldsymbol{\Psi}}_r - \boldsymbol{\Psi}_r\right)^*\right\}. \quad (25)$$

The derivative of the Lyapunov function candidate must be negative:

$$\dot{V} = \mathrm{Re}\left\{\left(\hat{\boldsymbol{\Psi}}_r - \boldsymbol{\Psi}_r\right)(d/dt)\left(\hat{\boldsymbol{\Psi}}_r - \boldsymbol{\Psi}_r\right)^*\right\} < 0. \quad (26)$$

The derivative of rotor flux error is obtained using (1) and (2).

$$(d/dt)\left(\hat{\boldsymbol{\Psi}}_r - \boldsymbol{\Psi}_r\right) = \Delta\boldsymbol{u}_s - \Delta L_s (d/dt)\boldsymbol{i}_s - \Delta R_s \boldsymbol{i}_s + \hat{\boldsymbol{\Psi}}_r u_m. \quad (27)$$

Stability condition yields to

$$\dot{V} = \mathrm{Re}\left\{\left(\hat{\boldsymbol{\Psi}}_r - \boldsymbol{\Psi}_r\right)\left(\hat{\boldsymbol{\Psi}}_r C_r\left(\hat{\Psi}_{PM} - \left|\hat{\boldsymbol{\Psi}}_r\right|\right)\right)^*\right\} < 0. \quad (28)$$

By using trigonometric functions for rotor flux description and when the amplitude of the rotor flux is known ($\hat{\Psi}_{PM} = \Psi_{PM}$), the condition becomes:

$$-C_r\left|\hat{\boldsymbol{\Psi}}_r\right|\left(\left|\hat{\boldsymbol{\Psi}}_r\right| - \hat{\Psi}_{PM}\right)\left(\left|\hat{\boldsymbol{\Psi}}_r\right| - \hat{\Psi}_{PM}\cos\left(\hat{\Theta} - \Theta\right)\right) < 0. \quad (29)$$

If rotor flux angle error is sufficiently small and C_r is positive, the condition is negative, therefore, the observer is stable within given restrictions (Urlep *et al.*).

5. SIMULATION RESULTS

The recursive matrix-based model of the three phase inverter, was used for simulations of the designed control algorithm in MATLAB/Simulink environment. A PMSM Iskra AMG 6308 with following parameters: R_s=0.15 Ω, L_s=237 mH, Ψ_{PM}=0.02 Vs, p=6, U_n=48 V, P_n=0.8 kW was used. The scope of the simulation was to control the PMSM in the speed mode using the PI speed-controller and proposed EDCC and to check the inverter response. The current controller outputs are the signals for the control of transistors. Fig. 4 shows the simulation results at the reference speed 500 1/min. The drive is started without load and accelerates to the reference speed. At the time 0.03s load is applied to the drive. The current controller successfully follows the referenced values.

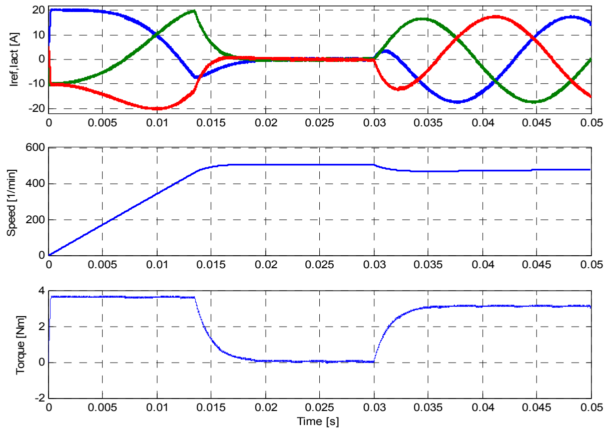

Fig. 4: Simulation results: phase currents (top), speed (middle) and torque (bottom).

6. EXPERIMENTAL RESULTS

Experimental setup was configured to verify the simulation results. It is implemented on in house developed experimental board, which includes Texas Instruments DSP TMS320C32 floating point DSP and Xilinx XCS40PQ240 FPGA (Fig. 5).

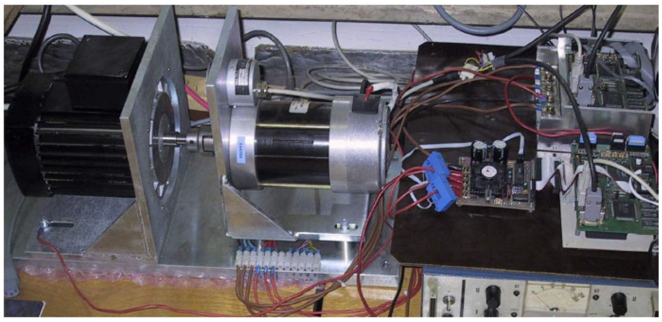

Fig. 5: Experimental setup.

The speed control algorithm and sliding-mode rotor flux observer of the PMSM are implemented on the DSP processor coded in C language, where algorithm execution time was set to the switching period 166 μs.

The switching current control is designed and implemented in FPGA. The algorithm is designed as DES and described using local vectors and matrices. Both the DES matrices and algorithm, formalized as shown in Fig. 1 and Fig. 2, are included directly in the VHDL code for FPGA (Fig. 6). FPGA also hosts the implementation of the interface for measurement of the phase voltages and two phase currents.

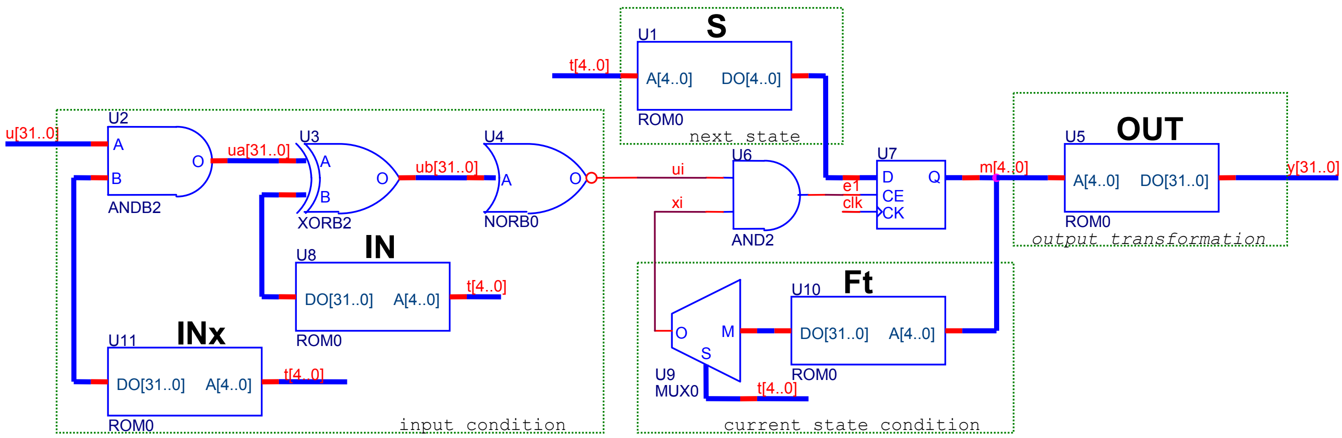

Fig. 6: Matrix logic controller mapping to the schematic of FPGA.

The phase current error is calculated and converted into logical conditions of DES algorithm using comparators with hysteresis, which is also implemented in FPGA (Fig. 1).

A/D conversion is the most critical operation of the switching current controller regarding time takes 2.7 µs. According to the fact, that A/D conversion takes most of the calculation time, while the calculation of the current error, hysteresis comparators and DES algorithm take less than 166 ns. The proposed approach replaces usual sequential calculation of algorithms on the DSP by parallel executable FPGA hardware.

Fig. 7 shows the speed response during speed reversing at low speed with constant load.

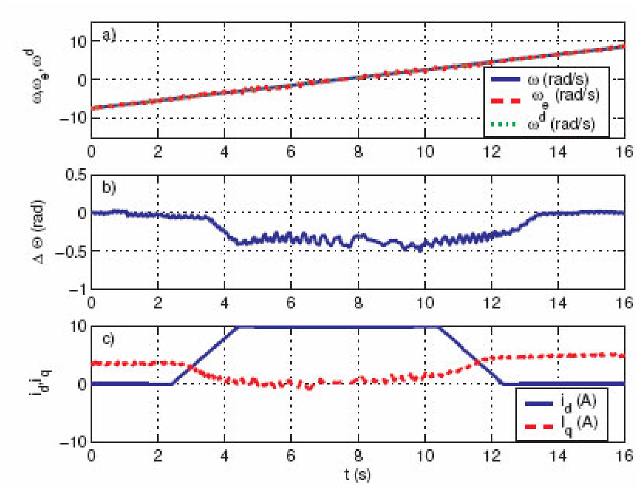

Fig. 7: Speed response during speed reversing at 1 rad/s^2 and T_l = 0.9 Nm with additional current i_d a), estimated angle error b) and reference currents.

7. CONCLUSION

This paper presents a speed sensorless VSS control of PMSM, based on both discontinuous and continuous sliding mode control principle. A discontinuous control in the form of discrete-event stator current control is used and implemented on the FPGA to achieve high frequency spectrum control and smooth torque response of machine. Another principle, a discrete time continuous sliding mode is employed in rotor flux observer. Due property of sliding mode principle the control is robust to parameter and load torque variation. The simulation and experimental results confirm the simplicity and robustness of the proposed control structure.

REFERENCES

Bolognani, S., Oboe, R. and Zigliotto, M. (1999). Sensorless Full-Digital PMSM Drive with EKF Estimation of Speed and Rotor Position. *IEEE Tran. Ind. Electronics,* **46**, no. 1, pp.184-191.

Edelbaher, G., Jezernik, K. and Urlep, E. (2006). Low-Speed Sensorless Control of Induction Machine. *IEEE Tran. Ind. Electronics,* **53**, no. 1, pp. 120-129.

Holtz, J.(2006) Sensorless Speed and Position Control of Induction Motors. In: *Tutorial, Proc. of 32-nd Annual Conference of the IEEE IES*, IECON, Paris.

Leonhard, W. (2001). *Control of Electrical Drives*. Springer-Verlag.

Polic, A. and Jezernik, K.(2005): Matrix based Event-Driven Approach for Current Control design of VSI. In: Proc. of ISIE'05, Dubrovnik. pp. 917-922, Piscataway, New Jersey, IEEE.

Rossi, C. and Tonielli, A.(1998). Robust Current Controller for Three-Phase Inverter using Finite State Automation. *IEEE Tran. Ind. Electronics*, **42**, no. 2, pp. 169-178.

Tilli, A. and Tonielli, A.(1998). Sequential Design of Hysteresis Current Controller for Three-Phase Inverter. *IEEE Tran. Ind. Electronics*, **45**, no. 5, pp. 771-781.

Urlep, E. and Jezernik, K.(2006). Speed Sensorless Variable Structure Control of PMSM. In: Proc. of 32-nd Annual Conference of the IEEE IES, IECON, Paris. 6p., Piscataway, New Jersey, IEEE.

Utkin, V. I.(1993). Sliding Mode Control Design Principles and Applications to Electric Drives. *IEEE Tran. Ind. Electronics*, **40**, no. 1, pp. 23-26.